AD-A150 580 IMPLICATIONS OF NOISE SOURCE RESOLUTION ON DETECTION PERFORMANCE FOR HORI..(U) NAVAL RESEARCH LAB WASHINGTON DC R M HEITMEYER ET AL. 07 FEB 85 NRL-8863 1/1

UNCLASSIFIED F/G 17/1 NL

END
FILMED
DTIC

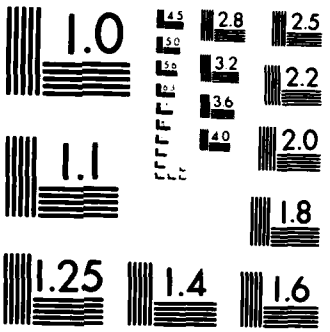

MICROCOPY RESOLUTION TEST CHART
NATIONAL BUREAU OF STANDARDS 1963 A

(2)

NRL Report 8863

AD-A150 580

Implications of Noise Source Resolution on Detection Performance for Horizontal Directional Systems Operating in Ship-Induced Noise Fields

R. M. HEITMEYER, L. J. DAVIS, AND N. YEN

Large Aperture Acoustics Branch
Acoustics Division

February 7, 1985

DTIC FILE COPY

DTIC
ELECTE
FEB 26 1985
S D
E

NAVAL RESEARCH LABORATORY
Washington, D.C.

Approved for public release; distribution unlimited.

3

AD-A150580

SECURITY CLASSIFICATION OF THIS PAGE

REPORT DOCUMENTATION PAGE

1a REPORT SECURITY CLASSIFICATION UNCLASSIFIED	1b RESTRICTIVE MARKINGS
2a SECURITY CLASSIFICATION AUTHORITY	3 DISTRIBUTION/AVAILABILITY OF REPORT Approved for public release; distribution unlimited.
2b DECLASSIFICATION/DOWNGRADING SCHEDULE	
4 PERFORMING ORGANIZATION REPORT NUMBER(S) NRL Report 8863	5 MONITORING ORGANIZATION REPORT NUMBER(S)
6a NAME OF PERFORMING ORGANIZATION Naval Research Laboratory — 6b OFFICE SYMBOL (If applicable) 5160	7a NAME OF MONITORING ORGANIZATION
6c ADDRESS (City, State, and ZIP Code) Washington, DC 20375-5000	7b ADDRESS (City, State, and ZIP Code)
8a NAME OF FUNDING/SPONSORING ORGANIZATION Naval Electronic Systems Command — 8b OFFICE SYMBOL (If applicable) 612	9 PROCUREMENT INSTRUMENT IDENTIFICATION NUMBER
8c ADDRESS (City, State, and ZIP Code) Washington, DC 20360	10 SOURCE OF FUNDING NUMBERS PROGRAM ELEMENT NO 62759N; PROJECT NO; TASK NO XF59-552-100; WORK UNIT ACCESSION NO DN480-045

11 TITLE (Include Security Classification)
Implications of Noise Source Resolution on Detection Performance for Horizontal Directional Systems Operating in Ship-Induced Noise Fields

12 PERSONAL AUTHOR(S)
Heitmeyer, R.M., Davis, L.J., and Yen, N.

13a TYPE OF REPORT	13b TIME COVERED	14 DATE OF REPORT (Year, Month, Day)	15 PAGE COUNT
Interim	FROM _____ TO _____	1985 February 7	27

16 SUPPLEMENTARY NOTATION

17 COSATI CODES			18 SUBJECT TERMS (Continue on reverse if necessary and identify by block number)		
FIELD	GROUP	SUB-GROUP	Beam noise	Ship-induced noise field	Detection opportunity
			Array gain	Directivity	Ship resolution gain
			Linear array	Probability of detection	Noise model

19 ABSTRACT (Continue on reverse if necessary and identify by block number)

This report develops relationships between the probability of detection and the system and environmental factors governing the extent to which individual noise sources are angularly resolved by a linear array operating in a ship-induced noise field. The effect of noise source resolution is described both in terms of a "detection opportunity probability" and a "ship resolution gain" (SRG). The detection opportunity function describes the probability of detecting a constant level signal in a ship-induced noise field as a function of the mean signal excess. The SRG represents the change in the single-to-noise ratio required to achieve a specified detection probability for a ship-induced noise field over that required for a noise field with constant mean power. The results are obtained by using a model that relates the beam noise cumulative distribution function to the directivity and the side lobe level degradation of the system and to both the strength and the anisotropy of the shipping distribution. These results indicate that only a small increase in the directivity or a small decrease in the shipping strength can result in a large increase

(Continues)

20 DISTRIBUTION/AVAILABILITY OF ABSTRACT ☒ UNCLASSIFIED/UNLIMITED ☐ SAME AS RPT ☐ DTIC USERS	21 ABSTRACT SECURITY CLASSIFICATION UNCLASSIFIED
22a NAME OF RESPONSIBLE INDIVIDUAL Richard M. Heitmeyer	22b TELEPHONE (Include Area Code) (202)-767-2261 — 22c OFFICE SYMBOL 5160

DD FORM 1473, 84 MAR — 83 APR edition may be used until exhausted. All other editions are obsolete

SECURITY CLASSIFICATION OF THIS PAGE

19. ABSTRACT (Continued)

in the detection opportunity probability for a negative signal excess, and a large increase in the SRG for small detection probabilities. Furthermore, when the shipping is only weakly resolved, large degradations in the side lobe levels can be tolerated without an appreciable degradation in the SFG; when the shipping is highly resolved, any degradation in the side lobe level results in a corresponding degradation in the SRG. Moreover, a larger side lobe degradation can be tolerated for beams pointing in high noise directions than for beams pointing in low noise directions.

CONTENTS

1. INTRODUCTION 1
2. DETECTION OPPORTUNITY PROBABILITY 2
3. NOISE MODEL ASSUMPTIONS 5
4. THE ZERO SIDE LOBE CASE 9
5. THE DETECTION OPPORTUNITY FUNCTION 12
6. THE SHIP RESOLUTION GAIN 16
7. SUMMARY AND CONCLUSIONS 21
8. ACKNOWLEDGMENTS 22
9. REFERENCES 22

Accession For
NTIS GRA&I ☒
DTIC TAB ☐
Unannounced ☐
Justification
By
Distribution/
Availability Codes
Dist | Avail and/or Special
A-1

DTIC COPY INSPECTED

IMPLICATIONS OF NOISE SOURCE RESOLUTION ON DETECTION PERFORMANCE FOR HORIZONTAL DIRECTIONAL SYSTEMS OPERATING IN SHIP-INDUCED NOISE FIELDS

1. INTRODUCTION

The design and deployment of horizontal directional array systems require a thorough understanding of the effect of aperture length on the detection probability for the prevailing noise environment. For all ambient noise environments, increasing the aperture length increases the array gain, and hence, the beam-former output signal-to-noise ratio (S/N), thereby increasing the probability of detection. However, for arrays operating in ship-induced noise environments where the noise results from point sources distributed throughout the basin, there is an additional dependence on aperture length. In particular, increasing the aperture length increases the extent to which the strong noise sources are angularly resolved. For a given beam, this increases the prevalence of the time periods when no strong noise sources contribute to the beam power. During these periods, the beam noise is low relative to the mean, so that signals with a low mean S/N may be detected that might not otherwise be detected were it not for the increased noise source resolution. Similarly, increasing the noise source resolution increases the prevalence of the periods when a single strong source dominates the beam power. During these periods, the noise is high relative to the mean, so that signals with a high mean S/N that might be detected if the noise source were not angularly resolved, may no longer be detected. Thus, for ship-induced noise fields, increasing the aperture length affects detection performance not only by increasing the array gain, but also by increasing the extent to which noise sources are resolved.

The extent of the noise source resolution depends not only on array length, but also on the distribution of the shipping, the beam pattern side lobe level, and the acoustic transmission loss function. For fixed array length, steering direction and frequency, and hence fixed beamwidth, the noise source resolution should be greater under light shipping conditions than under heavy conditions because a few ships lie within the beamwidth a greater percentage of the time. Furthermore, a system with badly degraded side lobes should have less noise source resolution than one without side lobe degradation. The power from all the ships in the side lobe directions adds to that from the ships in the main lobe direction, thereby reducing the extent of the fluctuations. Similarly, the noise source resolution should be less when the shipping is concentrated in the side lobe regions than when the main lobe points in a low shipping direction since the fraction of the power due to ships in the side lobe region is larger. Finally, the range and bearing dependence of the acoustic transmission function should affect the noise source resolution since the contributions from ships in certain regions will be attenuated while the contributions of ships in other regions will be accentuated.

This report develops a methodology for both quantifying the effect of noise source resolution on detection performance and for relating that performance to characterizations of the system and the noise environment. Section 2 develops the underlying methodology. The effect of noise source resolution on detection performance is described in terms of both a "detection opportunity function" and a "ship resolution gain" (SRG). The detection opportunity function describes the probability of detecting a constant level signal in a ship-induced noise field as a function of the mean signal excess. This function, together with the probability density of the beam signal, is sufficient to determine the detection probability for a fluctuation signal in a ship-induced noise field. The SRG represents the change in the S/N required to achieve a specified detection probability for a ship-induced noise field over that

Manuscript approved September 11, 1984.

required for a noise field with constant mean power. As such, it represents an additional term in the sonar equation due to the noise source resolution of a ship-induced noise field.

Both the detection opportunity function and the SRG depend on the system parameters and the noise environment through the cumulative distribution of the ship-induced beam noise. This report characterizes this dependence by using a beam noise model described in Heitmeyer, Yen, and Davis [1] with the additional restriction that the mean transmission loss function is independent of range and bearing over the region of nonzero shipping. The system is described in terms of three parameters: the directivity, the side lobe-to-main lobe mean power ratio for an ideal system without side lobe degradation, and the degradation in the side lobe level relative to the ideal system. The shipping is described in terms of two parameters—"a main lobe shipping strength" and a "shipping anisotropy." The main lobe shipping strength specifies the mean number of ships per degree bearing in the direction of the main lobe. The shipping anisotropy represents the average number of ships in the main lobe sector relative to that in the side lobe sector. The formal definitions of these quantities, together with the expression for the beam noise cumulative distribution function, are presented in Section 3.

In Section 4, the properties of both the detection opportunity function and the ship resolution gain are developed for the case of a degenerate system where the beam pattern is zero in the side lobe sector. For this case, the detection opportunity function and the ship resolution gain depend only on the directivity and the main lobe shipping strength. As such, they provide a reference for the more realistic case of systems with a nonzero side lobe response operating in anisotropic shipping environments. The notion of weakly resolved and highly resolved noise fields is also defined for later use in classifying the properties of nondegenerate systems.

The properties of the detection opportunity function and the ship resolution gain for the nondegenerate system are determined in Sections 5 and 6. In Section 5, approximate expressions are developed which relate the detection opportunity function for the nondegenerate case to that for the zero side lobe case. Both the integrity of these approximations and the salient features of the detection opportunity function are illustrated through examples obtained using the exact expressions. In Section 6 the properties of the ship resolution gain are developed and illustrated for a Hann-shaded array and a detection opportunity probability of 10%. The summary and conclusions are presented in Section 7.

2. DETECTION OPPORTUNITY PROBABILITY

Consider a detection algorithm operating on the time averaged, beam-former power output. We assume that both the mean noise power and the signal power are approximately constant over each averaging period, but that both fluctuate slowly from one averaging period to another. This is certainly reasonable for ship-induced noise fields provided the averaging time is short compared to the time required for the ship bearings to change significantly with respect to the beam width. In addition, we assume that the signal and noise fields are independent and that the probability laws governing both are such that the detection performance for each averaging period depends only on the S/N. Under these assumptions a detection transition function, PD_∞, can be defined that represents the probability of detection as a function of the S/N for a fixed false alarm probability. Alternatively, the detection performance can be expressed as a function of the signal excess (SE) in terms of the transition function, $PD_\infty(\mathrm{SE}) = PD_\infty(\mathrm{SE} + \mathrm{RD})$, where the recognition differential (RD) is defined by $PD_\infty(\mathrm{RD}) = 0.5$, and the signal excess is determined by $\mathrm{SE} = \mathrm{S/N} - \mathrm{RD}$. These functions are easily computed when the noise field is Gaussian with zero mean and the signal field has either a constant level or is also Gaussian with zero mean. Finally, it is assumed that, over the total observation period of interest, the S/N is statistically stationary with probability density function, $P_{\mathrm{S/N}}$. Under these assumptions the detection probability for a fixed false alarm probability can be obtained according to

$$Pd = \int_{-\infty}^{\infty} PD_\infty(x) P_{\mathrm{S/N}}(x + RD)\, dx. \tag{2.1}$$

In this formulation, the S/N represents the fluctuations in the "mean" signal and noise powers pertaining to each averaging interval. Specifically, the S/N is defined as

$$S/N_t = BS_t - BN_t, \tag{2.2}$$

where $BN_t = 10 \log (BN_t')$ with BN_t' the mean noise power for a single averaging interval. The power BS_t is similarly defined in terms of BS_t'. (Throughout this report we use an apostrophy to indicate that a variable is expressed in a linear scale as opposed to a decibel scale.) The mean S/N for the total observation period is defined by

$$S/N = 10 \log (\overline{BS_t'}/\overline{BN_t'}), \tag{2.3}$$

where "—" denotes the mean value pertaining to the total observation period. With this definition, the S/N_t can be written in terms of "normalized" signal and noise powers (BS and BN) according to

$$S/N_t = BS - BN + S/N, \tag{2.4}$$

where $BN' = BN_t'/\overline{BN_t'}$, with a similar expression defining the normalized signal power BS. Note that in this formulation, S/N is not equal to the expected value to S/N, since the mean of the normalized powers on a decibel scale exceeds 0 dB, even though their means on a linear scale are unity.

The desired result is obtained by first expressing $P_{S/N}$ in terms of the probability densities of its constituents. In particular, from Eq. (2.4) and the independence assumption, it follows that $P_{S/N}$ can be written as

$$P_{S/N}(S/N_t) = \int_{-\infty}^{\infty} P_{BS}(b)\ P_{BN}(b + S/N - S/N_t)\text{dB}, \tag{2.5}$$

where P_{BS} and P_{BN} are the densities of the normalized signal and noise powers. Finally, by substituting Eq. (2.5) into Eq. (2.1) we obtain

$$PD(SE) = \int_{-\infty}^{\infty} P_{BS}(b)\ PD_o(b + SE)\ \text{dB}, \tag{2.6a}$$

where the mean signal excess (SE) is defined by

$$SE = S/N - RD, \tag{26b}$$

and

$$PD_o(SE) = \int_{-\infty}^{\infty} PD_\infty(x)\ P_{BN}(SE - x)\ dx. \tag{2.6c}$$

The function PD_o is referred to here as the detection opportunity function.

Equation (2.6) provides a methodology for isolating the effects on detection performance of the system attributes (array gain and recognition differential), the mean signal and noise powers, and the fluctuations in the signal and the noise powers. Figure 1 illustrates the functional relationships underlying this methodology. The properties of the detection algorithm are summarized in the detection transition function. This function describes the probability of detection for a fixed false alarm probability as a function of the signal excess when the mean power of both the signal and the noise is constant. The fluctuations in the beam noise power that occur over the observation period are described by the probability density of the normalized beam power. This density, together with the detection transition function, determines the detection opportunity function through the convolution integral of Eq. (2.6c). The detection opportunity function represents the probability of detecting a signal with constant mean power in the presence of noise fluctuations as a function of the mean signal excess. This interpretation follows from Eq. (2.6) since, for a constant level signal, P_{BS} is a delta function centered at 0 dB, and hence, $PD(SE) = PD_o(SE)$. The fluctuations in the beam signal are described by the normalized beam signal probability density. This density and the detection opportunity function determine the detection performance as a function of the mean signal excess in terms of the detection function PD. Finally, the actual probability is obtained by determining the mean signal excess in terms of the recognition differential, the array gain, and the mean hydrophone S/N.

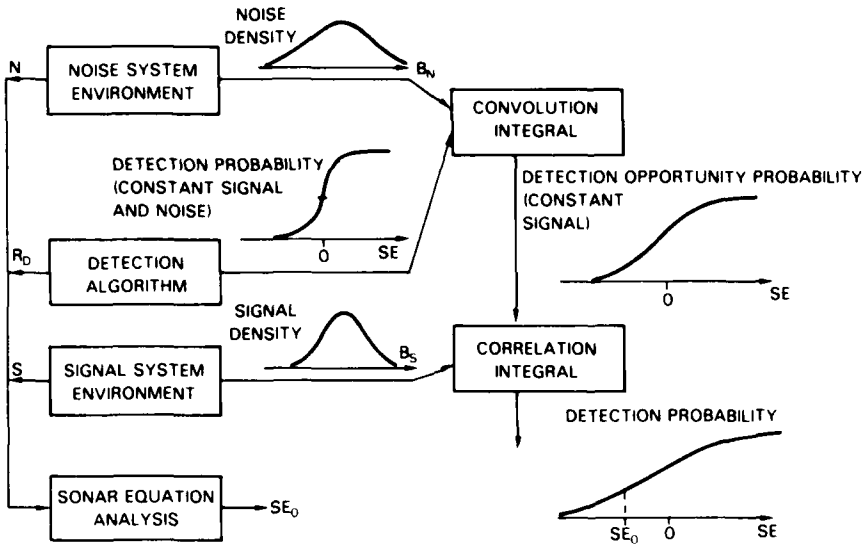

Fig. 1 — Detection performance analysis methodology

The relationships of Eq. (2.6) are consistent with the contention that, for a ship-induced noise field, increasing the noise source resolution increases the probability of detecting a low-level signal while decreasing the probability of detecting a high-level signal. This is seen through a qualitative interpretation of the effect of increased noise resolution on the detection opportunity function. In particular, for ship-induced noise fields the fluctuations in the beam noise are due to the passage of ships through the beam. Increasing the noise source resolution by reducing the beam width increases the fluctuations in both the beam noise and the spread in the beam noise probability density. An increased spread in the detection opportunity function results because of the convolution relationship of Eq. (2.6c). This in turn is equivalent to increasing the detection opportunity probability when SE is sufficiently negative and decreasing the detection opportunity probability when SE is sufficiently positive.

The effect of noise source resolution can also be described in terms of the change in the S/N required to achieve a specific detection probability. Specifically, for a fixed detection probability (PD) we define the "ship resolution gain" ($SRG(Pd)$) by

$$SRG(Pd) = SE_o - SE_c, \tag{2.7}$$

where SE_o and SE_c are the mean signal excess values determined by $Pd = PD_o(SE_o)$ and $Pd = PD_\infty(SE_c)$. The value SE_c is the mean signal excess required to achieve the detection opportunity probability (Pd) for a constant mean power noise field, whereas SE_o is the value required for a ship-induced noise field. Thus, their difference is the change in S/N required to obtain Pd. The detection performance will be improved or degraded by increased noise source resolution depending on whether the SRG is positive or negative.

We conclude by noting that for sufficiently long averaging times, both the detection opportunity function and the SRG can be obtained directly from the cumulative distribution function of the normalized beam noise. This follows because the interval over which the detection transition function goes from near zero to near unit probability decreases as the averaging time increases. The detection transition function can be approximated by a step function with transition at zero signal excess provided the desired false alarm probability is small. Making this approximation in the integral of Eq. (2.6c) results in

$$PD_o(SE) = F_{BN}(SE), \tag{2.8}$$

where F_{BN} is the probability distribution of the normalized beam noise. As a practical matter, Eq. (2.8) is an approximation which is reasonable when the spread in the beam noise density is large compared to the "transition interval" in the detection transition function.

Equation (2.8) indicates that the detection opportunity function is approximately given by the normalized beam noise distribution expressed as a function of signal excess. When this is the case, the SRG is approximately determined by $Pd = F_B(-SRG)$, where for notational simplicity, we have dropped the subscript on the beam noise. These assumptions are made throughout this report.

3. NOISE MODEL ASSUMPTIONS

The beam noise model used in this report assumes the ships are distributed throughout the basin according to a nonhomogeneous Poisson process, and that the total beam power is obtained as the finite sum of the contributions from the individual ships. Under this assumption, an explicit representation for the characteristic function of the beam noise power can be obtained in terms of the spatial shipping distribution, the array beam pattern, the basin-to-point acoustic transmission function, and the source level distribution function. The beam noise characteristic function can then be Fourier transformed to give the probability density which, when integrated, yields the cumulative distribution function. The theory underlying this model is described in Heitmeyer, Yen, and Davis [1]. Other beam noise models based on the Poisson shipping assumption are described in Moll and Zeskind [2,3].

The beam noise model represents the total beam noise as the sum of the noise due to ships in the main lobe-bearing sector plus the noise due to ships in the side lobe-bearing sector. For this representation, the distribution function for the total normalized beam power (F_B) can be expressed in terms of three parameters, Mm, Ms, and Bsm, and two distribution functions, F_{Bmo} and F_{Bso}. The parameters Mm and Ms are the mean number of ships in the main lobe and side lobe sectors. The parameter Bsm is the ratio of the mean power from ships in the side lobe sector to that due to ships in the main lobe sector expressed in a decibel scale. This parameter is referred to here simply as the side lobe power ratio. Finally, $F_{Bmo}(q;Mm)$ is the distribution of the main lobe beam power for a fixed Mm, given that there is at least one ship present in the main lobe sector. The definition of $F_{Bso}(q;Ms)$ is analogous to that of $F_{Bmo}(q;Mn)$, and q is an independent variable.

With these definitions, the distributions for the normalized main lobe and side lobe powers (F_{Bm} and F_{Bs}) are given by

$$F_{Bm}(b) = P_{Mm} + (1 - P_{Mm})\, F_{Bmo}(b - Bm;Mm) \text{ and} \tag{3.1a}$$

$$F_{Bs}(b) = P_{Ms} + (1 - P_{Ms})\, F_{Bso}(b - Bs;Ms), \tag{3.1b}$$

and the distribution for the total normalized beam power is

$$\begin{aligned} F_B(b) = {} & P_{Mm}P_{Ms} + P_{Mm}(1-P_{Ms})\, F_{Bso}(b-Bs;Ms) + P_{Ms}(1-P_{Mm})\, F_{Bmo}(b-Bm;Mm) \\ & + (1-P_{Mm})(1-P_{Ms})\, F_C(b;Mm,\, Ms,\, Bsm), \end{aligned} \tag{3.2a}$$

where

$$F_C(b;Mm, Ms, Bsm) = \int_{-\infty}^{b-Bs} f_{Bso}(z;Ms)\, F_{Bmo}(b + 10\log[1 + Bsm'(1 - 10^{-(b-z)/10})];\, Mm)\, dz. \tag{3.2b}$$

In these equations, P_{Mm} and P_{Ms} are the probabilities that no ships are present in the main lobe and side lobe sectors. These probabilities are related to the ship means (Mm and Ms) according to

$$P_M = \exp[-M]. \tag{3.3}$$

The auxiliary parameters (Bm and Bs) are the mean powers for the main lobe and side lobe sectors normalized to the total mean power and expressed in a decibel scale. They are related to the side lobe power ratio by

$$Bm = -10 \log (1 + Bsm') \tag{3.4a}$$

and

$$Bs = Bsm - 10 \log (1 + Bsm'). \tag{3.4b}$$

Finally, the distribution F_C is referred to here as the convolution distribution since it is the distribution of the sum of the power from both sectors when the power from neither sector is zero.

The application of the beam noise model requires specification of the shipping distribution and the acoustic transmission function, along with the array beam pattern and the source level distribution. In the general model, the shipping is specified by a spatial distribution function that represents the mean number of ships-per-unit area that are distributed throughout the basin according to the Poisson process. The transmission function is represented by a deterministic component and a stochastic component. The deterministic component represents the "smooth" variations in the transmission function with range and bearing, whereas the stochastic component represents the fluctuations about the smooth component.

We restrict the generality of the beam noise model to obtain simple parametric descriptions of the system and the noise environment. The shipping distribution, although arbitrary in form, is viewed as describing shipping that is constrained to a region where the mean transmission function is independent of range and bearing. Physically, this might provide a first approximation to a shipping lane confined to a region where the sound channel depth is a decreasing function of range. Note that even though we assume the deterministic component to be independent of range and bearing, the contribution from each ship experiences a different transmission loss due to the fluctuating component. These fluctuations are assumed to be exponentially distributed. Secondly, a specific source level characteristic function is assumed throughout the analysis. Heitmeyer and others have used this characteristic function, specified in Ref. 1, in the analysis of measured beam noise distribution functions at low frequencies. Finally, the actual array beam pattern, both with and without side lobe degradation, is approximated with a two-valued representation that is constant over the main lobe and side lobe sectors. This approximation is reasonable for arrays with element spacings and weights chosen to maintain low side lobes.

The analytical consequences of these assumptions are twofold. First, the distributions F_{Bmo} and F_{Bso} in Eq. (4.1) and Eq. (4.2) can be replaced by a single distribution, $F_{Bo}(q\ ;M)$. This distribution describes the noise due to ships in either the main lobe or the side lobe sector for a fixed M, given at least one ship present in that sector. It is determined only by the distributions of the source level and the fluctuating component of the transmission function. Second, the "functional" parameters in the beam noise model, Mm, Ms, and Bsm, are related to the system and the noise environment through only five "physical" parameters. The system is described by three parameters: the directivity, the side lobe power ratio for the ideal system in an isotropic field, and the side lobe degradation relative to the ideal system. This particular choice of system parameters is motivated by the form of the beam noise distribution function. The two noise environment parameters, the "main lobe shipping strength" and the "shipping anisotropy," depend only on the shipping distribution. The definitions of these physical parameters and their relationship to the functional parameters are presented in the remainder of this section.

The system parameters specify a two-valued approximation to the actual beam pattern. This approximation is obtained by requiring both beam patterns to have the same array gain and the same side lobe power ratio for an isotropic noise field.

The approximation is determined as follows. Consider a system where the beam pattern is not degraded. Let $BAo(\theta, \theta s)$ be the beam pattern for the steering angle (θs) normalized to a maximum of unity, and let $BWo(\theta s)$ be the beam width, defined by

$$BWo = \int BAo(\theta, \theta s)\, d\theta. \tag{3.4}$$

The directivity index, representing the array gain for a plane wave signal reception and a noise field that is isotropic with the received power confined to the horizontal plane, is then given by

$$DI' = DWo/\Phi. \tag{3.5}$$

We seek an approximation to the beam pattern that is unity over the bearing sector subtended by the main lobe and that has a constant side lobe level (s_o) over the remaining bearings. Specifically, define a main lobe sector $(|BW)$ to be a bearing sector of angular width BW centered at the steering direction, and define a side lobe sector $(|BWs)$ to satisfy $\Phi = |BW \cup |BWs$. Then the two-valued approximation is of the form

$$\begin{aligned} BAIo(\theta, \theta s) &= 1 \quad \text{for } \theta \text{ in } |BW(\theta s) \\ &= s_o \quad \text{for } \theta \text{ in} |BWs(\theta s), \end{aligned} \tag{3.6}$$

where the width of the main lobe sector (BW) satisfies $BW = x\ BWo$ for some x less than unity.

The array gain and side lobe power ratio requirements provide the two conditions necessary to determine s_o and x. These conditions are obtained as follows. First, since the maximum of both the actual and the ideal beam patterns is unity, their array gains will be the same if their integrals are the same. Using Eq. (3.4) and Eq. (3.6), this requirement yields the condition

$$1 = x + s_o'(DI' - 1). \tag{3.7}$$

Secondly, from Eq. (3.6), the side lobe power ratio requirements will be satisfied if

$$Bsmio' = (DI'/x - 1)s_o', \tag{3.8}$$

where $Bsmio$ is the side lobe power ratio for the actual beam pattern in isotropic noise.

The ratio $Bsmio$ can be computed for a specific beam pattern using numerical integration with the beamwidth BWo determining the main lobe and the side lobe sectors. Equations (3.7) and (3.8) can then be solved for the parameters s_o and x. Specific computations indicate that, for the broadside beam of a Hann-shaded array operating at the design frequency $(c/2\lambda)$, $Bsmio$ is essentially independent of directivity over the range from 10 to 30 dB with a value of -32.8 dB. For this case, the value of x obtained is essentially unity, so that $BW \cong BWo$ and the side lobe level and the directivity are approximately related by

$$Bsmio \cong 10 \log (DI' - 1) + s_o. \tag{3.9}$$

The value of $Bsmio$ corresponding to the Hann-shaded array is assumed in all numerical examples presented in this report.

Next, consider the system with degraded side lobes. For systems where the degradation is due to channel-to-channel errors that are statistically independent, the average beam pattern, normalized to a maximum of unity, can be written in the form

$$BA(\theta, \theta s) = (1 - sd')BAo(\theta, \theta s) + sd'. \tag{3.10}$$

The relationship between the level sd and the errors giving rise to the degradation (phase and amplitude errors, element position errors, missing hydrophone elements, etc.) is, in general, determined by the probability density governing the errors and is not considered here.

The two-valued approximation for the degraded system follows immediately from Eq. (3.10) by replacing BAo by its approximation. The result is

$$B_{Al}(\theta, \theta s) = 1 \quad \text{for } \theta \text{ in} | BW \tag{3.11a}$$
$$= s \quad \text{for } \theta \text{ in} | BWs,$$

where the equivalent side lobe level s is related to s_o and sd by

$$s' = (1 - sd')s_o' + sd'. \tag{3.11b}$$

Furthermore, since the form of the approximation is identical to that for the ideal beam pattern, the side lobe power ratio for the degraded system Bsm is obtained from Eq. (3.9) with s_o replaced by s. Specifically,

$$Bsm = (s - s_o) + Bsmio, \tag{3.12}$$

where $(s - s_o)$ is the degradation in the side lobe level.

The two shipping parameters are defined in terms of an "angular shipping distribution" that specifies the mean number of ships per degree bearing relative to the array site. This function, denoted here by $Da(\theta s)$, has the property that its integral over any bearing sector equals the mean number of ships in that sector. It follows that the functional parameters Mm and Ms can be written as

$$Mm = \int_{|BW} Da(\theta)\, d\theta \text{ and} \tag{3.14a}$$
$$Ms = \int_{|BWs} Da(\theta)\, d\theta. \tag{3.14b}$$

The two shipping parameters are defined for a fixed steering direction; together with the array directivity, they determine Mm and Ms. The main lobe shipping strength is defined as the average of $Da(\theta)$ over the main lobe sector. Similarly, the shipping anisotropy is defined as the main lobe shipping strength divided by the average over the side lobe sector. Specifically, the main lobe shipping strength is defined by

$$DA(\theta s) = (1/BW) \int_{|BW} Da(\theta s) d\theta, \tag{3.15}$$

and the shipping anisotropy is defined as

$$A(\theta s)' = Da(\theta s)(\Phi - BW)/\int_{|BW_s} Da(\theta)\, d\theta. \tag{3.16}$$

Note that for systems with at least modest directivity, $DA(\theta s) \doteq Da(\theta s)$, and both $DA(\theta s)$ and $A(\theta s)$ are essentially independent of the directivity. Moreover, as the array length approaches infinity and DI approaches infinity, the correspondence between $DA(\theta s)$ and $Da(\theta s)$ becomes exact, and $A(\theta s)$ approaches a limiting value (A_∞) given by

$$A_\infty = MB/MI, \tag{3.17}$$

where $MI = 180\, DA(\theta s)$, and MB is the total number of ships in the basin. Finally, note that, when expressed on a decibel scale, the shipping anisotropy $(A(\theta s))$ is less than zero, greater than zero, or equal to zero, depending on whether θs is a low shipping direction, a high shipping direction, or an isotropic shipping direction.

It remains to determine the relationship between the three functional parameters and the five physical parameters. From Eq. (3.14) and the definitions of the directivity, the main lobe shipping strength, and the shipping anisotropy, it follows immediately that Mm can be written as

$$Mm = 180\, DA(\theta s)/DI' \tag{3.18}$$

and Ms can be written as

$$Ms = Msm\ Mm, \tag{3.19}$$

where

$$Msm = (DI' - 1)/A'. \tag{3.20}$$

The auxiliary parameter Msm is referred to as the side lobe shipping ratio.

To relate Bsm to the physical parameters, note that when the transmission function is independent of range and bearing over the region of nonzero shipping, the mean beam power for both the main lobe and the side lobe sectors is proportional to the mean number of ships in those sectors. It follows that for arbitrary shipping, $BSm' = s'Msm$. This fact, together with Eq. (3.20) and the definition of $Bsmio$, yields

$$Bsm = (s - s_o) - A(o\theta) + Bsmio. \tag{3.21}$$

The preceding equations indicate that for a fixed steering direction, the functional parameters can be expressed in terms of three system parameters, $Bsmio$, DI, and $(s - s_o)$, and two shipping parameters, $DA(\theta s)$ and $A(\theta s)$. The mean number of ships in the main lobe sector (Mm) is proportional to the main lobe shipping strength and inversely proportional to the directivity. The mean number of ships in the side lobe sector (Ms), is an increasing function of the directivity and a decreasing function of the side lobe shipping anisotropy. Finally, the side lobe power ratio (Bsm) is linearly related to the shipping anisotropy, the side lobe level degradation, and $Bsmio$.

4. THE ZERO SIDE LOBE CASE

For a beam pattern with zero side lobe response, the beam noise distribution function depends only on the distribution F_{Bo} and the parameter Mm. Specifically, from Eq. (3.1a) with $Bm = 0$, we have

$$F_{Bz}(b) = P_{Mm} + (1 - P_{Mm})\ F_{Bo}(b;\ Mm), \tag{4.1}$$

where the subscript "z" denotes the zero side lobe response case.

Equation (4.1) represents the distribution function as a sum of two terms. The first term (P_{Mm}) is the probability that no ships lie in the main lobe sector and, since it acts as a lower bound to the distribution, it also equals the probability of observing no noise. This is a consequence of the zero side lobe assumption since, for zero side lobes, the only ships that contribute to the noise are those that lie in the main lobe sector. Note that the first term depends only on Mm and hence on the directivity and the main lobe shipping strength through Eq. (3.3).

The second term represents the contribution from ships lying in the main lobe sector. The factor $(1 - P_{Mm})$ is the probability that at least one ship lies in the sector, and the distribution (F_{Bo}) is the beam noise distribution conditioned on at least one ship being present. This term depends not only on the directivity and the shipping strength through the parameter Mm, but also on the source level and transmission loss assumptions through their effect on F_{Bo}.

Equation (4.1) indicates that the character of the beam distribution function can be distinguished by whether or not P_{Mm} is significant. We refer to noise fields as highly resolved if $P_{Mm} > 0.1$, weakly resolved if $P_{Mm} < 0.02$, and partially resolved otherwise. For weakly resolved noise fields where P_{Mm} is negligible, the character of the distribution is essentially determined by $F_{Bo}(b;Mm)$. For highly resolved noise fields, the contribution of F_{Bo} is reduced by the factor $(1 - P_{Mm})$, and the constant term P_{Mm} in Eq. (4.1) becomes significant.

The extent of the noise field resolution can also be defined in terms of the parameter (Mm) or equivalently, in terms of the main lobe shipping strength and the directivity. In particular, the noise field is highly resolved if $Mm < 2.3$, weakly resolved if $Mm > 3.9$, and partially resolved otherwise. Equivalently, the field is weakly resolved if either $DA > DAw(DI)$, or $DI < DIw(DA)$ where

$$DAw = 10^{**}(DI - 16.64) \tag{4.2a}$$

and

$$DIw = 10 \log(DA(0s)) + 18.93. \tag{4.2b}$$

Similarly, the field is highly resolved if either $DA < DAh(DI)$, or $DI > DIh(DA)$ where

$$DAh = 10^{**}(DI - 18.93) \tag{4.3a}$$

and

$$DIh = 10 \log(DA(\theta s)) + 16.64. \tag{4.3b}$$

The parameter Mm is henceforth referred to as the noise resolution parameter.

The detection opportunity function for zero side lobe response ($PDoz$) is illustrated in Fig. 2 for selected values of Mm. This function is obtained by equating $PDoz$ to F_{Bz}. It is seen that a decrease in Mm, corresponding to an increase in the noise field resolution, results in an increased spread in the distribution function. More precisely, for negative values of b, $F_{Bz}(b)$ increases as Mm decreases, whereas for b sufficiently positive, $F_{Bz}(b)$ decreases with decreasing Mm. Physically, this indicates that an increase in the extent to which the noise field is resolved results in an increase in the prevalence of both the low noise and the high noise periods. In terms of the detection opportunity probability, this is equivalent to increasing $PDoz$ when the mean signal excess is negative, and decreasing $PDoz$ when SE is sufficiently positive.

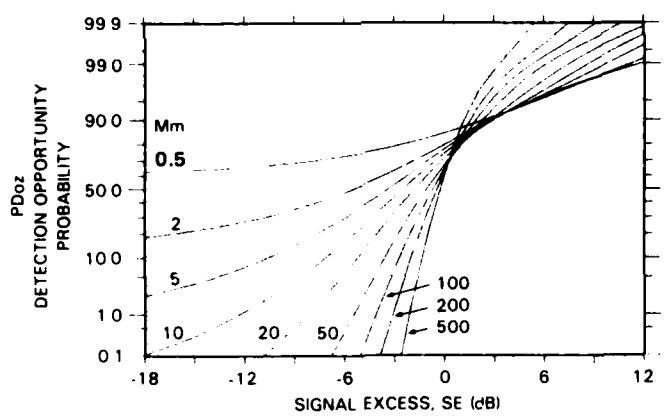

Fig. 2 — Detection opportunity functions for zero side lobes and Mm = 0.5, 2, 5, 10, 20, 50, 100, 200, 500 ships per beam

The detection opportunity functions for highly resolved noise fields in Fig. 2 correspond to Mm values of 0.5 and 2 ships per beam. As predicted by Eq. (4.1), these functions approach PMm as b approaches $-\infty$. In principle, if a zero side lobe response could be achieved, this probability would continue to increase towards unity as the array length and, hence, the system directivity, approached infinity. Were this the case, the beam distribution would approach unity for all finite values of the beam level and the detection opportunity probability would approach unity for all signal levels. In reality, the contribution to the noise due to the nonzero side lobe response of the beam pattern reduces the probability of observing extremely low beam noise levels to essentially zero as seen in Section 5.

Figure 3 shows the detection opportunity probability for selected values of the mean signal excess as a function of the noise resolution parameter. Each of these curves was obtained by fixing the value of b and plotting $F_{B_z}(b;Mm)$ as a function of Mm. The curve labelled "zero side lobe bound" represents a lower bound to the detection opportunity probability. This curve is the probability of observing no noise on the beam, $F_{B_z}(-\infty) = PMm$, and is hence the probability of detecting an arbitrarily small signal level. As seen from Eq. (3.3), this curve decreases linearly with $\log(Mm)$. The two curves corresponding to a negative SE, -10 and -3 dB, show a substantial increase in the detection opportunity probability as the noise field becomes highly resolved. This improvement results from the increased prevalence of the low noise periods due to the increased noise source resolution. In contrast, the curve for positive SE (3 dB) shows only a modest degradation in the detection opportunity as the noise field becomes highly resolved. In practical terms, the degradation for positive signal excess evident in Fig. 3 means that a signal that is visible almost all of the time for a constant power noise field will be visible only slightly less often, whereas the improvement for negative SE means that a signal that is only rarely visible will be visible a significant percentage of the time. Finally, the detection opportunity for $SE = 0$ dB lies everywhere above 0.5 and shows a gradual improvement for increased noise field resolution. Since 0.5 is the detection probability for a constant mean noise power, this indicates that performance is improved by the ability to resolve sources in a ship-induced noise field even out to very large values of Mm.

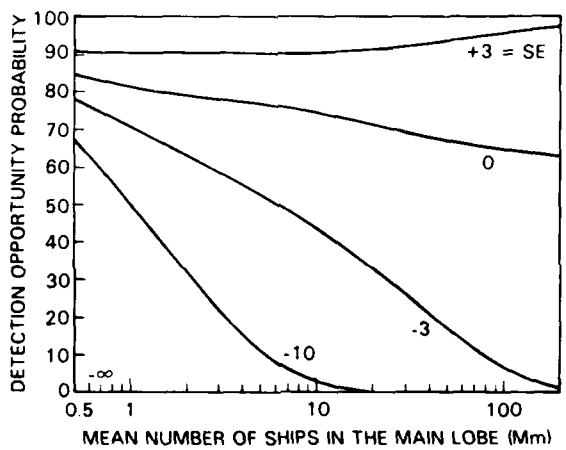

Fig. 3 — Detection opportunity probability vs Mm for zero side lobes and the mean signal excess, $SE = -\infty, -10, -3, 0, 3$ dB

Figure 4 illustrates the dependence of the shipping resolution gain on the extent of the noise field resolution for two values of the detection probability, $Pd = 0.1$ and 0.5. Both curves are obtained by numerically solving the equation, $F_{B_z}(-SRGz) = Pd$, for Mm such that $P_{Mm} < Pd$. For Mm such that $Pd > P_{Mm}$, there is no solution to the equation and $SRGz$ is infinite. In heuristic terms, for zero side lobes the percentage of time when no noise is observed exceeds Pd, and during these periods any nonzero signal level will be detected. The values of Mm for which the $SRGz$ becomes infinite are 0.69 and 2.3 ships per beam for Pd equal to 0.5 and 0.1.

Two features are evident in the $SRGz$ curves of Fig. 4. First, both curves show a dramatic increase with decreasing Mm. This increase corresponds directly to a reduction in the S/N required to achieve the detection probability as the noise resolution increases over that required for constant mean noise power fields. Secondly, the 10% $SRGz$ curve lies everywhere above the 50% $SRGz$ curve, indicating that the reduction in required S/N is largest for the smallest detection probability.

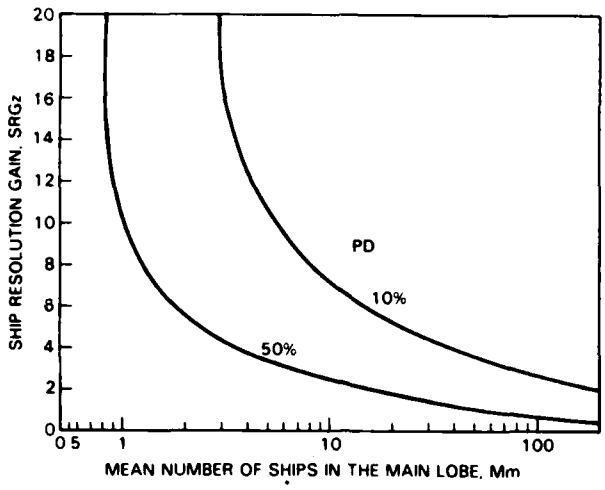

Fig. 4 — Ship resolution gain (SRG) vs *Mm* for zero side lobes and the detection probability, $Pd = 0.1$ and 0.5

5. THE DETECTION OPPORTUNITY FUNCTION

For realistic beam patterns where the side lobe response is not zero, the beam distribution function will depend on *Ms* and *Bsm* as well as *Mm*. In this section, we first develop two approximations for the general case. These approximations lead to expressions which relate the salient features of the detection opportunity function to the parameters *Mm*, *Ms*, and *Bsm*. Finally, this dependence is illustrated through computations obtained using the exact expression.

The first approximation yields an expression for the general distribution that is analogous to Eq. (4.1). This approximation results from restricting the mean number of ships in the side lobe region (Ms) to be sufficiently large so that $P_{Ms} = \exp[-Ms]$ can be approximated by zero in Eq. (3.2a). In particular, for $Ms > 5$, $P_{Ms} < 0.01$ and the error resulting from setting $P_{Ms} = 0$ in Eq. (3.2a) will be small. This approximation is applicable except under conditions of extremely light shipping or for systems of very low directivity. Neither of these conditions is of practical importance. For very light shipping, noise from other sources will dominate the ship-induced noise component. For low directivity systems, the side lobe level is not a critical performance parameter since most of the noise is due to shipping on the main lobe. Thus, for the cases of interest, the distribution is approximately given by

$$F_B(b) = P_{Mn}\, F_{Bo}(b - Bs; Ms) + (1 - P_{Mm})\, F_C(b;\, Mm,\, Ms,\, Bsm). \tag{5.1}$$

The interpretation of Eq. (5.1) is analogous to that of Eq. (4.1) for the zero side lobe case. For weakly resolved noise fields where P_{Mm} is negligible, the beam distribution is essentially given by the convolution distribution F_C. For highly resolved fields where both terms are significant, the first term no longer provides a lower bound since the distribution $F_{Bo}(b - Bs;\, Ms)$ goes to zero as b approaches $-\infty$. As seen from Eq. (3.1b), this distribution represents the contribution due to the nonzero side lobe response. By comparing Eq. (3.1b) with Eq. (4.1), this distribution can be obtained from the distributions of Fig. 2 by identifying *Ms* with *Mm* and shifting by *Bs*. For later reference, note from Eq. (3.4b) that when $Bsm < -6$ dB, *Bs* is essentially equal to *Bsm* so that the shift is essentially linear in *Bsm*.

The second approximation results in an expression relating the convolution distribution to the distribution F_{Bo}. This approximation applies when the ratio of the standard deviation of the side lobe contribution to that of the main lobe contribution is much less than unity. In this case, the integration in

Eq. (3.2b) can be approximated by replacing the density F_{Bo} by a delta function centered at the mean value of $10 \log(1 - PMs)$. This results in

$$F_C(b;\, Mm,\, Ms,\, Bsm) \cong F_{Bo}(b + g(b,\, Bsm);\, Mm) \qquad \text{for } b > Bs \tag{5.2a}$$
$$\cong 0 \qquad \text{for } b < Bs,$$

where

$$g(b,\, Bsm) = 10 \log\, [(1 + 10^{Bsm/10})\, (1 - 10^{-b/10})], \tag{5.2b}$$

and we have assumed P_{Ms} to be unity. Reference 1 shows that the approximation condition can be written as

$$Bsm < -10 + 5 \log(Msm), \tag{5.3}$$

where we have used 0.1 as an upper bound on the standard deviation ratio. Note that within the limits of the approximation condition, the convolution distribution depends only on Mm and Bsm and not on Ms. Furthermore, for weakly resolved fields, Eq. (5.2) provides an approximation to the total beam noise distribution since, according to Eq. (5.1), F_C can be identified with F_B when P_{Mm} is negligible.

The preceding approximations provide the basis for determining the dependence of the distribution F_B on the side lobe power ratio Bsm when the convolution approximation is satisfied. We begin by using the convolution approximation to determine the relationship between F_C and F_{Bo}. To this end, note for Eq. (5.2b) that for fixed Bsm, g is an increasing function of b that approaches $10 \log(1 + Bsm')$ as b approaches infinity, and is zero for $b = 0$. Furthermore, for fixed b, g is also an increasing function of Bsm. These observations, together with the fact the F_{Bo} is an increasing function of b, indicate that for $b \leqslant 0$, F_C is a decreasing function of Bsm that is bounded above by $F_{Bo}(b;\, Mm)$. For $b \geqslant 0$, $F_C(b,\, Mm,\, Bsm)$ is an increasing function of Bsm that is bounded below by $F_{Bo}(b;\, Mm)$ and bounded above by $F_{Bo}(b + 10 \log(1 + Bsm');\, Mm)$.

For weakly resolved fields, the results are obtained by identifying F_{Bz} with F_{Bo} and F_B with F_C. The inequalities between F_C and F_{Bo} then become

$$F_B(b;\, Mm,\, Bsm) \leqslant F_{Bz}(b;\, Mm) \qquad \text{for } b \leqslant 0, \tag{5.4a}$$

$$F_{Bz}(b;\, Mm) \leqslant F_B(b;\, Mm,\, Bsm) < F_{Bz}(b + 10 \log(1 + Bsm');\, Mm) \quad \text{for } b \geqslant 0. \tag{5.4b}$$

The implications of Eq. (5.4) are threefold. First, for a nonzero side lobe response, the prevalence of both the negative noise periods and the positive noise periods can be no more than that obtained with a zero side lobe response. This follows from Eq. (5.4a) and the first inequality in Eq. (5.4b). Secondly, the prevalence of both the negative noise periods and the positive noise periods decreases when either the side lobe degradation increases or the shipping anisotropy decreases. This follows from Eq. (3.21) together with the fact the F_B is a decreasing function of Bsm for negative b, and an increasing function of Bsm for positive b. Finally, whereas the decrease in the prevalence of the negative noise periods can be substantial, the decrease in the positive noise periods is not significant for reasonable side lobe degradations and shipping anisotropies. This follows since according to Eq. (5.4b), F_B is essentially equal to F_{Bz} as long as Bsm is reasonably small. In particular, if $Bsm < -6$ dB, the upper bound in Eq. (5.4b) is obtained from the lower bound by a shift to the left of less than 1 dB. For the Hann-shaded array, this condition is satisfied as long as the side lobe degradation plus the shipping anisotropy is less than -26.8 dB.

The preceding results can be stated in terms of the detection opportunity function as follows. For negative SE, an increase in Bsm resulting from an increase in either the side lobe degradation or a decrease in the shipping anisotropy will decrease the detection opportunity probability. Furthermore, for negative SE, the detection opportunity probability can never exceed that obtained with a zero side lobe response. Conversely, for positive SE, an increase in Bsm increases the detection opportunity and

$PDoz(SE)$ constitutes a lower bound. However, for positive SE, the increase in PDo is small for reasonable side lobe degradations and shipping anisotropies.

For highly resolved fields, identical results for F_B and PDo can be obtained only when b is negative unless an additional constraint is imposed on Bsm. To establish the results for negative b, it suffices to show that F_B is a decreasing function of Bsm and that Eq. (5.4a) holds. Equation (5.1) shows that F_B decreases with Bsm since increasing Bsm both shifts $F_{Bo}(b - Bs; Ms)$ to the right and decreases F_C. Furthermore, Eq. (5.4a) holds since for $b \leqslant 0$, $F_B \leqslant P_{Mm} + (1 - P_{Mm})F_C \leqslant P_{Mm} + (1 - P_{Mm})F_{Bo} = F_{Bz}$. For positive b, the results will follow only if Bsm is sufficiently positive so that $F_{Bo}(b - Bs; Ms)$ is essentially zero for $b > 0$. When this is the case, $F_B \leqslant P_{Mm} + (1 - P_{Mm})F_C$ for $b > 0$. Thus, F_B increases with increasing Bsm since F_C increases with Bsm and Eq. (5.4b) follows from the inequalities for F_C and F_{Bo}.

The approximations of Eq. (5.1) and Eq. (5.2) also yield expressions for the SRG for both the highly resolved and the weakly resolved noise fields. These expressions provide an alternate description of the effect of Bsm on the detection opportunity function in terms of the value of the signal excess required to achieve a given Pd. The approximation for the highly resolved field is obtained from Eq. (5.1) as follows. Assume $P_d < P_M$ and that Bs is small enough so that the two terms in Eq. (5.1) separate; e.g., the range of b where $F_{Bo}(b; Mm)$ is approximately zero overlaps the range of b where $F_{Bo}(b - Bs; Ms)$ is approximately unity. Then the condition defining the SRG, $Pd = F_B(-SRG)$, is essentially equivalent to the condition $P_d = P_{Mm}F_{Bo}(-SRG - Bs; Ms)$. It follows that

$$SRG(Pd; Mm, Ms, Bsm) = SRGo(Pd/P_M; Ms) - Bsm + 10\log(1 + Bsm'), \tag{5.5}$$

where $SRGo(P; M)$ is defined by $P = F_{Bo}(-SRGo(P; M); M)$.

The SRG approximation for weakly resolved fields is obtained from Eq. (5.2). Let $SRGo$ and $SRGc$ be the ship resolution gains associated with the distributions F_{Bo} and F_C. By definition, these gains satisfy $F_{Bo}(-SRGo) = P_d = F_C(-SRGc)$ so that from Eq. (5.2a), we must have $SRGo = SRGc - g(-SRGc, Bsm)$. The result follows after substituting for g from Eq. (5.2b), solving for $SRGc$ in terms of $SRGo$, and identifying $SRGc$ with $SRGo$. Specifically,

$$SRG(Pd; Mm, Ms, Bsm) = SRGo(P_d; Mm) - DSRG(P_d; Mm, Bsm), \tag{5.6a}$$

where the degradation in the ship-resolution gain due to nonzero side lobe response ($DSRG$), is given by

$$DSRG(Pd; Mm, Bsm) = 10\log[1 + 10^{(Bsm + SRGo)/10}] - 10\log[1 + 10^{Bsm/10}]. \tag{5.6b}$$

Equations (5.5) and (5.6) can be used to relate the tails of the detection opportunity function (PDo) to those of PDz when Bsm is sufficiently small. Note that for both the highly resolved and the weakly resolved fields, $SRGo$ can be identified with $SRGz$ since in both cases the parameter M in $SRGo(P_d; M)$ is assumed large enough so that $F_{Bo} = F_{Bz}$. For the weakly resolved field, Bsm must be small enough to satisfy the approximation condition, whereas for the highly resolved field, Bsm must be small enough for the two distributions to separate.

To illustrate the above properties and to determine the behavior when the approximation condition is not satisfied, representative distributions have been computed using the exact formulation. Figures 5 and 6 illustrate the corresponding detection opportunity functions for a weakly resolved field ($Mm = 10$) and a highly resolved field ($Mm = 0.5$). The two plots of each figure show functions for different values of the side lobe shipping ratio: a low value ($Msm = 10$ dB) shown in the left plot, and a high value ($Msm = 30$ dB) shown in the right plot. The different functions in each plot were computed for a range of side lobe power ratios increasing from −15 dB to 5 dB in 5 dB increments. Also shown is the function for zero side lobes for comparative purposes. Note that for $Msm = 10$ dB, the

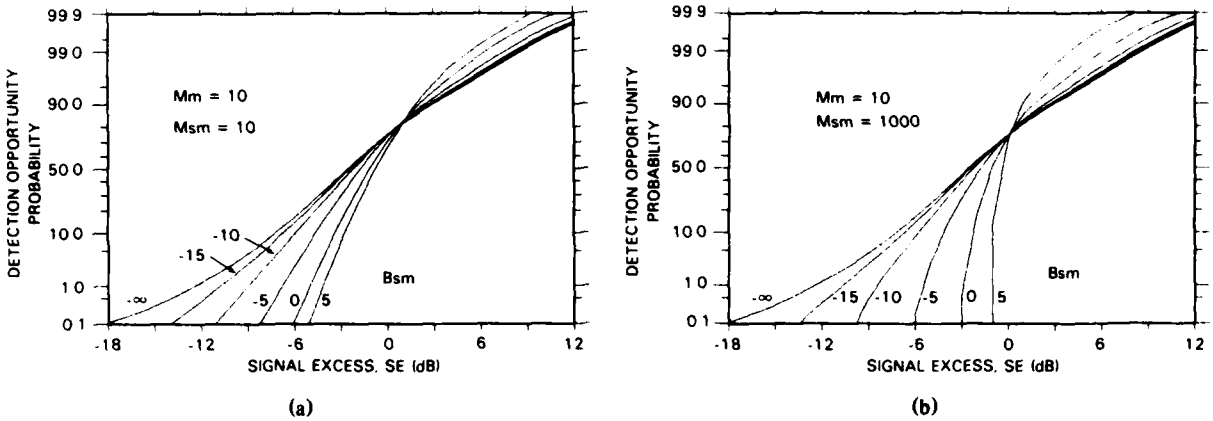

Fig. 5 — Detection opportunity functions for $Mm = 10$, $Bsm = -15, -10, -5, 0, 5$ dB. Left plot, $Msm = 10$ dB; right plot, $Msm = 30$ dB.

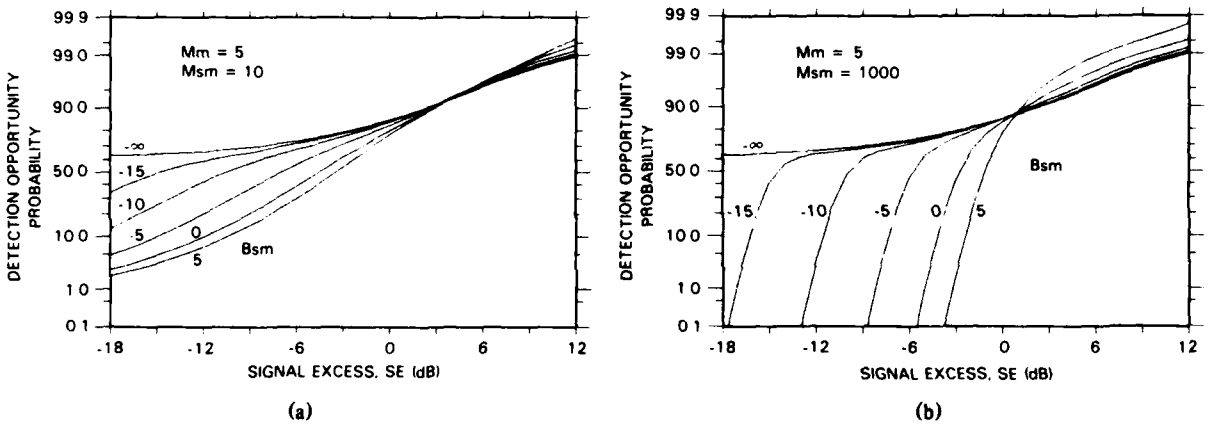

Fig. 6 — Detection opportunity functions for Mm −0.5, $Bsm = -15, -10, -5, 0, 5$ dB. Left plot $Msm = 10$ dB; right Plot $Msm = 30$ dB.

functions for $Bsm \leqslant -5$ dB satisfy the convolution approximation condition, whereas for $Msm = 30$ dB, all the functions satisfy the approximation condition. Thus, the comparison of the functions for $Bsm = 0$ and 5 dB in the left plot with the corresponding functions in the right plot illustrates the dependence on Msm when the approximation condition is not satisfied.

An examination of the detection opportunity functions for the weakly resolved field of Fig. 5 supports the integrity of the approximation properties when the approximation condition is satisfied. As expected, the functions for $Bsm = -15, -5$, and 0 dB are essentially equal in both plots even though the side lobe ratio (Msm) differs by 20 dB. Furthermore, the upper tails of the −15 and −10 dB functions are indistinguishable from the upper tail of the zero side lobe function, and only a slight increase in the upper tail of the −5 dB function is evident. Finally, the shift in the lower tails of each of the functions for $Msm = 30$ dB is consistent with that predicted by Eq. (5.5). This is seen by substituting the value of SRG_z (7.2 dB), into Eq. (5.5b) to obtain degradation values of 0.5, 1.4, 3., 5., and 6.3 dB as Bsm increases from −15 to 5 dB. These values correspond very closely to the degradations seen in the functions of the lower plot.

The character of the detection opportunity function when the approximation condition is not satisfied is illustrated by the 0 and 5 dB functions in Fig. 5a, and in the comparison of these functions with the corresponding functions in Fig. 5b. Two features are evident in the inspection and comparison of these functions. First, Fig. 5a shows that for fixed *Msm*, the lower tail continues to decrease and the upper tail continues to increase with increasing *Bsm*. Secondly, the comparison between Figs. 5a and 5b shows that for fixed *Bsm*, the decrease in the lower tail and the increase in the upper tail are less than that obtained when the approximation condition is satisfied.

The detection opportunity functions for the highly resolved noise field are shown in Fig. 6. In each plot the lower tails of the functions are essentially shifted replicas of one another. This is expected since the lower tail of the beam distribution is dominated by the side lobe distribution and its form is invariant for *Mm* and *Msm* fixed. Direct evidence of this dominance is seen in the comparison of the form of the lower tails with that of the side lobe distribution obtained from Fig. 2 by identifying *Ms* with *Mm*. In particular, for the functions of Fig. 6b where $Msm = 1000$ and hence $Ms = 500$, the lower tails are almost identical in form to that of the $Mm = 500$ distribution of Fig. 2. Similarly, the lower tails of the functions of Fig. 6a where $Msm = 10$ and thus $Ms = 5$ agree well in form with the $Mm = 5$ distribution of Fig. 2. Finally, note that the shifts in the lower tails of the functions are in very good agreement with those predicted by Eq. (5.5) with *Bs* related to *Bsm* by Eq. (3.4b). The single exception occurs for the 0 and 5 dB functions in Fig. 6a where the separation condition leading to Eq. (5.5) is not satisfied for the small value *Msm*.

6. THE SHIP RESOLUTION GAIN

The ship resolution gain characterizes the effect of noise source resolution in terms of the reduction in the S/N required to achieve a particular detection opportunity probability. In this section, we develop the properties of the SRG for a fixed detection opportunity probability of 10%, and relate those properties to the system parameters DI and s, and the shipping parameters $DA(\theta s)$ and $A(\theta s)$.

The dependence of the *SRG* on the functional parameters is illustrated in Fig. 7. Each curve shows the 10% *SRG* as a function of the noise field resolution parameter. The side lobe parameters for each plot are the same as those for the detection opportunity function plots of the preceding section. An inspection of these curves indicates that for fixed *Bsm*, the *SRG* increases with increasing noise field resolution and, for fixed *Mm*, the *SRG* decreases with increasing *Bsm*. Furthermore, for weakly resolved fields ($Mm > 3.9$) the *SRG* is essentially independent of *Msm*, whereas for highly resolved fields ($Mm < 2.3$) the *SRG* decreases for increasing *Msm*.

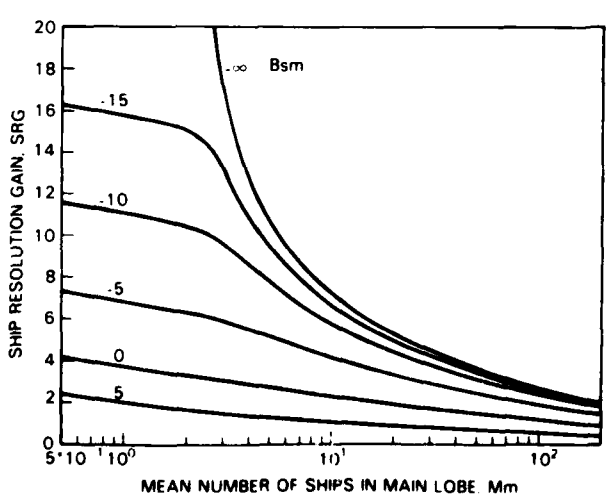

Fig. 7 — Ship resolution gain (SRG) vs *Mm* for *Bsm* = −∞, −15, −10, −5, 0, 5 dB

The interpretation of these characteristics in terms of the physical parameters is as follows. For weakly resolved fields where $DA(\theta s)$ or DI satisfy Eq. (4.2), the SRG increases gradually with either increasing DI or decreasing $DA(\theta s)$. Moreover, the SRG for the hypothetical, zero side lobe beam pattern ($SRGz$) provides an upper bound, and the SRG approaches $SRGz$ slowly with decreasing Bsm. This indicates that a substantial degradation in the side lobe level can be tolerated without an appreciable degradation in the SRG.

For partially resolved fields, the SRG exhibits a significant increase as Mm decreases from 3.9 to 2.3. In terms of the directivity, this indicates that an increase in the directivity of less than 2.3 dB can result in a major reduction in the S/N required for a 10% detection probability. This improvement is due only to the improved noise source resolution and is in addition to the 2.3 dB improvement resulting from the increased array gain. In terms of the main lobe shipping strength, this same improvement can result when the main lobe shipping strength is reduced by a factor of 1.7.

Finally, for highly resolved fields where $DA(\theta s)$ or DI satisfies Eq. (4.3), the SRG increases approximately in inverse proportion to $\log(Mm)$. For fixed DI, this indicates that the SRG is a decreasing function of the main lobe shipping strength that approaches infinity as $DA(\theta s)$ approaches zero. This follows since Mm is the only parameter determined by $DA(\theta s)$. On the other hand, for fixed DA the SRG approaches a finite limit as the DI approaches infinity as seen later in the section. In either case, the SRG decreases essentially linearly with increasing Bsm, indicating that either an increase in the side lobe degradation or a decrease in the shipping anisotropy results in a corresponding decrease in the SRG.

For the weakly resolved field, it remains only to determine the dependence of the SRG degradation on the side lobe degradation and the shipping anisotropy. To this end, Eq. (5.6) can be solved to determine an upper bound on Bsm, $Bsma$, such that the SRG degradation is is less than a prescribed amount ($DSRGa$) whenever Bsm is less than $Bsma$. Equation (3.21) can then be used to relate the allowable side lobe degradation and the shipping anisotropy to $Bsma$. This procedure results in the condition: if $(s - s_o) < (s - {}_o)a$, then $SRG > SRGz(Mm) - DSRGa$, where the allowable side lobe degradation, $(s - s_o)a$, satisfies

$$(s - s_o)a - A(o\theta) < Bsma(Mm) - Bsmoi, \tag{6.1a}$$

and the allowable side lobe power, $Bsma(Mm)$, is given by

$$Bsma(Mm) = 10 \log[(1 - 10^{-DSRGa/10})/(10^{(SRGz(Pd;Mm)-DSRGa)/10} - 1)]. \tag{6.1b}$$

According to Eq. (6.1), the allowable side lobe degradation depends only on the shipping anisotropy and on the directivity and shipping strength through Mm. For fixed DI and $DA(\theta s)$ and hence fixed Mm, $(s - s_o)a$ increases in high shipping directions and decreases in low shipping directions in inverse proportion to the shipping anisotropy. Alternatively, for fixed $A(\theta s)$, $(s - s_o)a$ is a decreasing function of DI and an increasing function of $DA(\theta s)$. This follows since $SRGz$ is a decreasing function of Mm and hence, $Bsma$ is an increasing function of Mm. Note also that these results are independent of Msm since they are based on Eq. (5.6) with the assumption that the approximation condition, Eq. (5.3), is satisfied.

Both the dependence of the allowable side lobe degradation on Mm and the integrity of Eq. (6.1) can be seen from the plots of $Bsma(Mm)$ in Fig. 8. The two curves shown were computed by numerically evaluating the SRG to determine $Bsma(Mm)$ for a $DSRGa$ of 1 dB with Msm fixed at 30 dB and 10 dB. The bound determined from Eq. (6.1b) is essentially the same as the 30 dB curve and is not shown. The integrity of Eq. (6.1) is supported by the comparison of the two curves since there is only a small increase in $Bsma$ as Msm is decreased from 30 dB to 10 dB. The strong dependence of $(s - s_o)a$ on Mm is evidenced by the strong dependence of $Bsma(Mm)$ seen in the curves. As a numerical example for a Hann-shaded array ($Bsmio = -32.8$ dB) operating in isotropic shipping

($A(\theta s) = 0$ dB), the allowable side lobe degradation required to restrict the *SRG* to within 1 dB of *SRGz* increases from 10.5 dB to 29.1 dB as *Mm* increases from 3 to 100 ships per beam.

For the highly resolved field, it remains to determine the dependence of the *SRG* on the system directivity as well as on the side lobe degradation and the shipping anisotropy. To this end, we first determine an expression for the limit of the *SRG* as the *DI* approaches infinity. This expression is obtained from Eq. (5.5) using Eq. (3.21) to relate *Bsm* to the side lobe degradation and the shipping anisotropy as *DI* approaches infinity. In particular, Eq. (3.17) shows that $A'(\theta s)$ approaches MI/MB as *DI* approaches infinity. Thus *Bsm* approaches $(s - s_0)_\infty + 10\log(MI/MB) + Bsmio$ where $(s - s_0)_\infty$ is the limit of the side lobe degradation. Furthermore, the first term of Eq. (5.5) approaches $SRGo(Pd, MB)$ as *DI* approaches infinity since *PMm* approaches unity and *Ms* can be written as $MI(DI' - 1)/(DJ'A')$. Thus the *SRG* approaches

$$SRG_\infty = SRGo(P_d; MI/A_{\infty'}) - Bsm_\infty + 10\log(1 + Bsm_{\infty'}), \tag{6.2a}$$

where the limiting side lobe power ratio, Bsm_∞, is given by

$$Bsm_\infty = (s - so)_\infty - A_\infty + Bsmio, \tag{6.2b}$$

and A_∞ is determined by Eq. (3.17). Note that for realistic main lobe shipping strengths, $MB = MI/P\infty'z$ will be large enough so that $SRGo(P_d; MB) \sim SRGz(P_d; MB)$, in which case the curves of Fig. 2 can be used to evaluate the first term in Eq. (6.2a). Also, when $Bsm_\infty < -6$ dB, the last term in Eq. (6.2a) is essentially zero.

Equation (6.2) specifies the *SRG* for an array of infinite length with an arbitrary shipping environment and side lobe degradation. For this hypothetical array, the dependence of the *SRG* on the shipping parameters and the side lobe degradation follows from Eq. (6.2). In particular, it is seen that a decrease in $(s - s_0)_\infty$ results in a corresponding decrease in SRG_∞. Furthermore, the *SRG* decreases as the main lobe shipping strength increases since $SRGz(P_d, MI)$ is a decreasing function of $DA(\theta s)$. Finally, the *SRG* is larger in a high shipping direction than in a low shipping direction. This follows since both the first and the third terms in Eq. (6.2) are increasing functions of A_∞. This remains true even if the total shipping (MB) is held constant since, although the first term remains constant, the third term still increases with increasing A_∞.

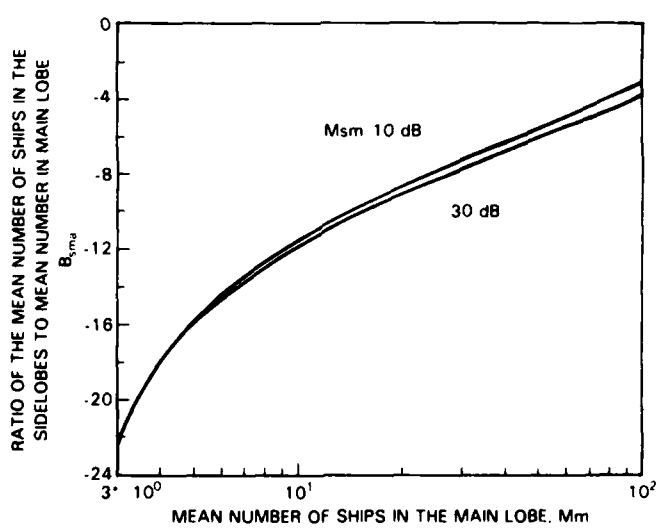

Fig. 8 — Bound on the side lobe power ratio, *Bsma*, necessary to restrict the SRG degradation to 1 dB for *Msm* = 10 and 30 dB

The limiting *SRG* provides a reference against which the *SRG* for a finite length array can be compared for different main lobe shipping strengths, shipping anisotropies, and side lobe degradations. Two issues remain: is the *SRG* for a finite array an increasing function of the directivity and, if so, how fast does the *SRG* approach SRG_∞? If the *SRG* increases with *DI*, then any increase in *DI* due to either an increase in array length or a change in the beam steering direction will increase the *SRG* provided *Bsm* remains constant. Furthermore, if the *SRG* converges slowly to SRG_∞, then large increases in the directivity, beyond that required to highly resolve the noise field, are required to achieve near maximum *SRG*; whereas, rapid convergence implies that only small increases in the *DI* are necessary to achieve near maximum performance. In Figs. 9 to 12, these issues are examined through direct computation of the *SRG* as a function of the directivity for selected values of the main lobe shipping strength, the side lobe degradation, and the shipping anisotropy.

Figure 9 shows the *SRG* directivity curves for selected main lobe shipping strengths when the side lobe degradation is zero and the shipping is isotropic. Each of these curves was obtained with *Bsm*, Bsm_∞, and *Bsmio* identically equal to −32.8 dB. The five main lobe shipping strengths increase from 0.5 to 8 ships per degree in powers of two. From Eq. (4.2a) and Eq. (4.3a), the directivity needed to highly resolve the noise field (*DIh*) increases in 3 dB increments from 16 dB to 28 dB, and is 2.3 dB larger than *DIw*. Furthermore, for *DA* = 0.5 ships per degree, *MB* is ninety so that, from Fig. 3, *SRGo*(0.1; *MB*) is about 3 dB. It follows from Eq. (6.2a) that SRG_∞ is almost 36 dB. For the remaining shipping strengths, SRG_∞ decreases slightly since *SRGo*(0.1; *MB*) decreases slightly as *DA* increases.

Two features are evident in the curves of Fig. 9. First, each curve shows a dramatic increase in the *SRG* as the directivity increases from the maximum value for which the noise field is weakly resolved (*DIw*) to the minimum value for which the noise field is highly resolved (*DIh*). In particular, using the appropriate values of *DIw* and *DIh* for each main lobe shipping strength, it is seen that the *SRG* increases by over 15 dB as the *DI* increases by 2.3 dB from *DIw* to *DIh*. This supports the earlier observation that small increases in the directivity or small decreases in the shipping strength can dramatically improve the *SRG* performance.

Second, not only does the *SRG* continue to increase towards SRG_∞ for highly resolved fields, but only small increases in the *DI* beyond *DIh* are necessary to achieve near maximum *SRG*. In particular, for each curve it is seen that SRG_∞ is no more than 6 dB larger than the *SRG* for a directivity of *DIh*, and that an increase in the *DI* by 3 dB reduces the difference to less than 2 dB.

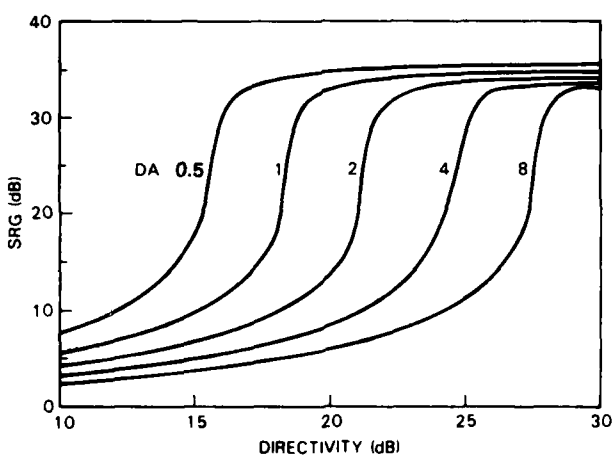

Fig. 9 — Ship resolution gain (SRG) vs directivity (DI) for isotropic shipping zero side lobe degradation, and main lobe shipping strengths, *DA* = 0.5, 1., 2., 4., 8. ships per degrees

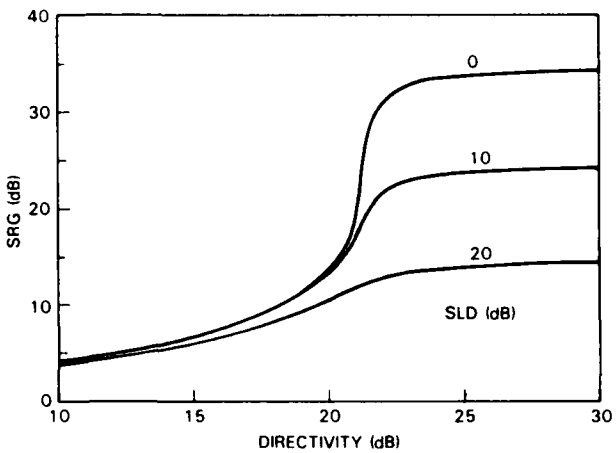

Fig. 10 — Ship resolution gain (SRG) vs directivity (DI) for isotropic shipping, a shipping strength of 2 ships per degree, and side lobe degradations, *SLD* = 0, 10, 20 dB

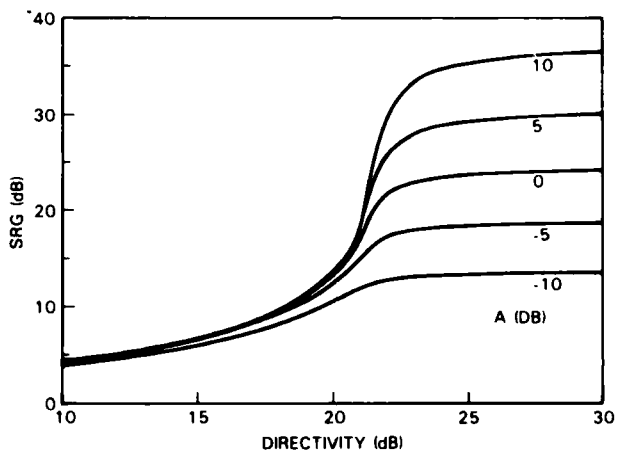

Fig. 11 — Ship resolution gain (SRG) vs directivity (DI) for a shipping strength of 2 ships per degree, a side lobe degradation of 10 dB, and shipping anisotropies, $A = -10, -5, 0, 5, 10$ dB

Fig. 12 — Ship resolution gain (SRG) vs directivity (DI) for isotropic shipping, a shipping strength of two ships per degree, and side lobe levels $s = -20, -25, -30, -30, -35, -40, -45$

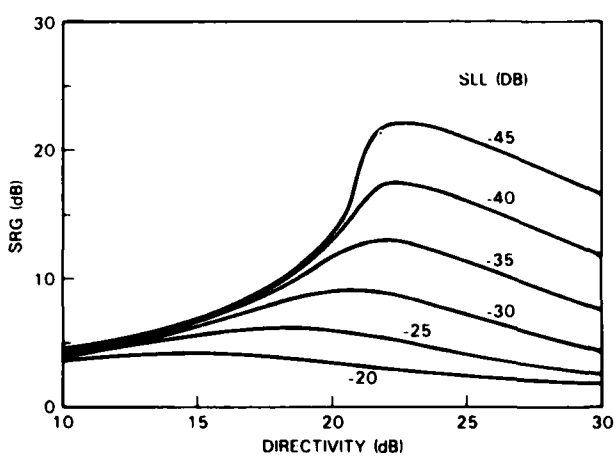

Figures 10 and 11 show *SRG* directivity curves for a fixed main lobe shipping strength and selected side lobe degradations and shipping anisotropies. In both figures, note again that once the field is highly resolved, near maximum *SRG* is obtained with a modest increase in directivity. Furthermore, the dependence of the limiting *SRG* on the side lobe degradation and the shipping anisotropy is in agreement with that predicted by Eq. (6.2). In Fig. 10, where the shipping anisotropy is 0 dB, the decrease in the limiting *SRG* is essentially equal to the increase in the side lobe degradation. In Fig. 11, where the side lobe degradation is fixed at 10 dB, the difference between the limiting *SRG* for anisotropic shipping and that for isotropic shipping decreases slightly as the anisotropy decreases. Furthermore, this difference is always larger than the anisotropy. This behavior is consistent with Eq. (6.2) since the first term is both positive and an increasing function of the anisotropy.

The curves of Fig. 11 indicate that the *SRG* is larger when the mainbeam is in a high shipping direction than when it is in a low shipping direction. It is emphasized that this does not indicate that the overall detection performance is improved by operating in a high shipping direction, since the array gain will be smaller than for a low shipping direction, and this will compensate for the increased *SRG*.

We conclude by emphasizing that the limiting *SRG* of Eq. (6.2) need not be an upper bound if *Bsm* depends on the directivity. This is evidenced in the curves of Fig. 12, where the side lobe level (s) rather than the side lobe degradation is held constant as the directivity increases. An inspection of these curves indicates that when the side lobe degradation does not remain constant, the *SRG* performance actually decreases as the directivity approaches infinity. This behavior is consistent with Eq. (6.2) since, for a constant side lobe level, $(s-s_0)_\infty$ approaches $-\infty$ as *DI* approaches ∞.

7. SUMMARY AND CONCLUSIONS

This report has developed a methodology for analyzing the detection performance of horizontal directional systems operating in ship-induced noise fields. The noise effects are described in terms of both a detection opportunity function and a ship resolution gain. These quantities, together with the array gain and the beam signal distribution function, determine the detection probability through Eq. (2.6). The properties of these quantities have been developed using a particular beam noise model with the assumption that the mean transmission loss function is independent of range and bearing over the region of nonzero shipping.

The results indicate that for a negative signal excess the detection probability can be considerably larger for a ship-induced noise field than for a constant mean power noise field, whereas for a positive signal excess the detection probability should be only slightly smaller. Furthermore, increasing the aperture length can result in a significant improvement in the detection opportunity probability for a low-signal excess at the expense of a modest decrease for a high-signal excess. For a negative-signal excess, the largest improvement in the detection opportunity probability occurs when the aperture length is increased from the point where the field is weakly resolved to the point where the field is highly resolved. Equations (4.2) and (4.3) specify the increase in the system directivity required to obtain this improvement.

The analysis of the ship resolution gain indicates that small increases in the directivity or small decreases in the shipping strength can dramatically improve the *SRG* performance. In particular, the examples illustrate that the *SRG* can increase by over 15 dB as the *DI* increases by 2.3 dB, or alternatively, as the main lobe shipping strength decreases by a factor of 1.7. Furthermore, increasing the system directivity beyond the point where the noise field is highly resolved does not appreciably increase the *SRG*. Finally, the effect of side lobe degradation and shipping anisotropy is critically dependent on whether the field is weakly resolved or highly resolved. For the weakly resolved noise field, a substantial degradation in the side lobe level can be tolerated without appreciably degrading the *SRG* performance. Equation (6.1) specifies the side lobe degradation that can be tolerated without a significant

degradation in the *SRG*. For the highly resolved field, any increase in either the side lobe degradation or decrease in the shipping anisotropy results in a corresponding decrease in the *SRG*.

It is emphasized that the actual numerical results presented here depend on the specific assumptions made in the noise model computations. A change in the source level distribution, which is frequency dependent, and the inclusion of range and bearing dependence in the mean transmission function can be expected to affect the numerical results. Nevertheless, it is reasonable to expect that the principles, if not the numerics, will extend to more realistic source and acoustic environmental models.

8. ACKNOWLEDGMENTS

The authors are grateful to Dr. Orest Diachok and Dr. Budd Adams for their many helpful discussions which were of major importance to this work.

9. REFERENCES

1. R. Heitmeyer, N. Yen, and L. Davis, "Properties of Beam Noise Distribution Functions for Ship-Induced Noise Fields," ASW Research Centre, in press.

2. M. Moll, R. M. Zeskind, and F. J. M. Sullivan, "Statistical Measures of Ambient Noise: Algorithms, Program, and Predictions," Report No. 3390, Bolt, Beranek and Newman, Inc., June 1977.

3. "Review of Models of Beam Noise Statistics," SAI-78-696-W/A, Science Applications, Inc., McLean, Va., Nov. 1977 [AD-A055 728].

END

FILMED

3-85

DTIC